Bacterial pathogens associated with the plastisphere of surgical face masks and their dispersion potential in the coastal marine environment

Jingguang Cheng, Pu Wang, Jean-François Ghiglione, Lu Liu, Zhonghua Cai, Jin Zhou, Xiaoshan Zhu

Bacterial pathogens associated with the plastisphere of surgical face masks and their dispersion potential in the coastal marine environment

***Authors**:* Jingguang Cheng[a], Pu Wang[a], Jean-François Ghiglione[b], Lu liu[a], Zhonghua Cai[a], Jin Zhou[a, *], Xiaoshan Zhu[a, c, **]

Affiliations:

[a] *Shenzhen International Graduate School, Tsinghua University, Shenzhen 518055, PR China*

[b] *CNRS, Sorbonne Université, Laboratoire d'Océanographie Microbienne (LOMIC), Observatoire Océanologique de Banyuls, Banyuls sur mer 66650, France*

[c] *College of Ecology and Environment, Hainan University, Haikou 570228, PR China*

Author information:

(**) Corresponding author:

Xiaoshan Zhu; Shenzhen International Graduate School, Tsinghua University, Shenzhen 518055, PR China. Email: zhu.xiaoshan@sz.tsinghua.edu.cn

* *Co-corresponding author:*

Jin Zhou; Shenzhen International Graduate School, Tsinghua University, Shenzhen 518055, PR China. Email: zhou.jin@sz.tsinghua.edu.cn

Abstract

Huge numbers of face masks (FMs) were discharged into the ocean during the coronavirus pandemic. These polymer-based artificial surfaces can support the growth of specific bacterial assemblages, pathogens being of particular concern. However, the potential risks from FM-associated pathogens in the marine environment remain poorly understood. Here, FMs were deployed in coastal seawater for two months. PacBio circular consensus sequencing of the full-length 16S rRNA was used for pathogen identification, providing enhanced taxonomic resolution. Selective enrichment of putative pathogens (e.g., Ralstonia pickettii) was found on FMs, which provided a new niche for these pathogens rarely detected in the surrounding seawater or the stone controls. The total relative abundance of the putative pathogens in FMs was higher than in seawater but lower than in the stone controls. FM exposure during the two months resulted in 3% weight loss and the release of considerable amounts of microfibers. The ecological assembly process of the putative FM-associated pathogens was less impacted by the dispersal limitation, indicating that FM-derived microplastics can serve as vectors of most pathogens for their regional transport. Our results indicate a possible ecological risk of FMs for marine organisms or humans in the coastal and potentially in the open ocean.

Keywords

Plastic debris; microplastic; Pathogen identification; Biofilm; Bacterial colonization

Environmental Implication

The majority of surgical face masks were made of polypropylene plastics in the form of fibers, which were frequently found in the tissue of marine organisms. They were considered persistent organic pollutants because of extremely low environmental degradation rates and toxicity to marine organisms. We showed that FMs could release considerable microfibers *in situ*, exacerbating the plastic pollution in the marine environment. The enrichment of specific pathogens on FMs and the elevated pathogens' dispersion potential indicates that the FMs or released microfibers can cause disease to marine organisms in the coastal and even a broader environment.

Graphical abstract

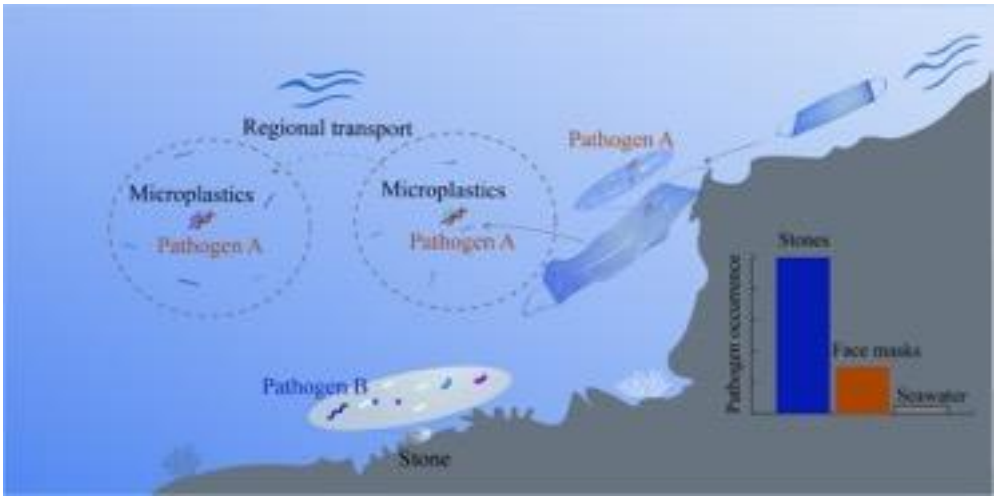

1. Introduction

The abrupt outbreak of coronavirus disease in 2019 (COVID-19) led to a global health crisis. Countermeasures were implemented to restrict the spread of the disease, such as wearing face masks (FMs), travel restrictions, and lockdowns [1], severely affecting life activities. Monthly FM consumption was estimated to reach 129 billion in 2020 [2]. However, extensive use and mismanagement of FMs caused a blooming threat to the fluvial and marine environment [3]. For example, FMs accounted for 9% of total floating debris from a river during the pandemic [4]. Considerable FMs can originate from the coast, where up to 100 pieces of FMs can be observed in a beach [5]. It is estimated that 0.39 million tons of FMs ended up in the ocean within a year during the pandemic [6].

Disposable FMs mainly consist of polypropylene microfibers [3]. Recent research demonstrated that an FM can release thousands of microplastics in seawater *versus* millions after a UV aging treatment [7–9]. The aging process of FMs was primarily performed within controlled laboratory environments. Indeed, once a piece of plastic enters the ocean, it can be rapidly colonized by marine microorganisms, such as bacteria and phytoplankton (e.g., diatoms), the so-called biofilm or plastisphere [10–12]. The biofilm formation can reduce the UV access to FMs, potentially retarding the aging process in the marine environment. Conversely, the water sheer stress [13] and bioerosion [14] can promote the release of microplastics/nanoplastics *via* fragmentation. Therefore, the aging process of FMs in the marine environment can be distinct from that in laboratory environments, which cannot be accurately evaluated without field exposure.

Microplastics in the fiber form (i.e., microfibers) in the marine environment can be particularly detrimental to marine animals. Microfiber was the main shape found in the marine fish, suggesting a blockage of their digestive tracts [15]. Other studies showed that

some additives (such as Mn, Zn, Ni, Pb, Cd, and Cr) and microplastics were toxic to marine life [16–18]. Over the past decade, intensive research was conducted to characterize the bacterial structure, assembly mechanisms, and environmental drivers of the plastisphere bacterial communities, for which the pathogens were of great concern [10]. In 2013, Zettler et al. investigated the plastisphere from the North Atlantic and described that the potentially pathogenic *Vibrio* dominated the bacterial community in a polypropylene sample [10]. A recent meta-analysis also showed that the putative pathogen Vibrionales and *Tenacibaculum* spp. were more abundant in the plastic samples than the control biofilm or the planktonic samples in the marine environment [19]. However, some other studies found that the putative pathogenic species were actually more abundant on natural substrates for members of genera *Arcobacter*, *Pseudomonas*, *Shewanella*, and *Vibrio* [20]. These methods are generally derived from second-generation sequencing of the 16S rRNA gene (less than 500 base pairs in general for the sequence length) [19–22], the higher taxonomic ranks, i.e., at the family level or the genus level, can contain many non-pathogenic species. For instance, the genus *Vibrio* comprises over one hundred species, only twelve of which are regarded as human pathogens [23]. Consequently, low resolution was the main drawback of pathogenic bacteria profiling for the second-generation sequencing, which makes it hard to assign the pathogens to the species level and, in turn, makes the pathogen results less relevant to the real condition. Even through decades of research, limited progress was achieved in this field. Moreover, to evaluate the pathogen threats to marine ecosystems, the host range at multiple trophic levels is needed to assess the pathogen risks to the marine environment instead of mainly focusing on the pathogens of human beings from previous studies.

In contrast to bacterial colonization behavior, bacteria can detach from the plastisphere, the so-called bacterial dispersion, i.e., bacteria escape from the biofilm structure, and both favorable (e.g., nutritional sufficiency) and unfavorable (e.g., oxygen depletion) conditions

can contribute to bacterial dispersion [24]. Previous studies showed that the bacterial community in the plastisphere was driven by the surrounding environmental conditions, indicating that during the microplastic transport, there could be bacterial recruitment from the surrounding seawater to the plastisphere and bacterial dispersal from the plastisphere to its surrounding seawater [25,26]. This raises the question as to whether pathogens from FM-derived microplastics will increase pathogen dispersal during their transport in the marine environment.

While fine microfibers of FMs make them susceptible to the ocean current, frictions can result in the FM breakdowns into microplastics. We hypothesized that the aging process of FMs will be retarded due to biofilm formation, FMs can selectively enrich pathogens, and the released microplastics can further promote pathogen dispersion in the marine environment. Here, surgical face masks were incubated in coastal seawater for two months to allow the development of a mature biofilm. Three stations were chosen to represent a gradient of human impacts, which also permitted the assessment of the pathogen dispersal potential. After the FM exposure, the change in the functional groups was tested using the Fourier transform infrared (FTIR) spectroscopy. In addition, the weight loss of the FMs was tested after a biofilm removal process. Scanning electron microscopy was employed to evaluate the change in surface roughness. To unveil the taxonomies of pathogens in a higher resolution, i.e., at the species level, the PacBio circular sequencing was adopted to characterize the full-length 16S rRNA sequences (around 1470 base pairs). Moreover, a custom-made pathogenic bacteria database was constructed, comprising the pathogen target at multiple trophic levels. This study aims to 1) test the FM deterioration in the marine environment, 2) characterize the pathogen profiles in the plastisphere, and 3) assess the dispersion potential of bacteria/pathogens in the plastisphere from a null model analysis. We aimed to understand

the pathogenic behavior and environmental risks during the aging process of masks and provide services for coastal ecological health/management.

2 Materials and Methods

2.1 Experimental setup

Commercially available surgical FMs were fixed inside polyethylene cages, which were fastened under water quality monitoring buoys at a water depth of around 0.5 m. Ordinary black agate stones were used as controls. The exposures were performed from Oct. to Dec. in 2021. Three locations along the coast of Shenzhen, China, were chosen to represent different anthropogenic influences, i.e., an open-water station situated 200 meters from the coast (114.567°E, 22.465°N), a bay with intensive aquaculture (114.515°E, 22.565°N), and a semi-enclosed bay of the metropolis (113.946°E, 22.477°N) (Figure 1). Pristine FMs were used in this study to avoid any heterogeneous absorbent materials after wearing.

After 2-month incubation, FMs, stones, and seawater were collected from the three stations. Before biofilm sampling, FMs and stones were rinsed with 0.2 μm filtered seawater using a spray bottle to remove loosely attached materials. FMs were aliquoted using a sterile scissor. Biofilm from the stones was scraped using sterile throat swabs. Besides, one liter of seawater was filtrated using 0.2 μm polycarbonate membrane filters (47 mm diameter, Nucleopore). Samples were performed in triplicates and stored at -80 ℃ after the treatments.

2.2 Weight loss and microplastic counting

For the weight loss assay, biofilm on FMs was removed with a nitric acid digestion process at 80 ℃ for 24 hours using a temperature-controlled hot plate (SINEO, China) [27]. After

digestion, FMs were washed with ten cycles of the ultrasonic bath with preheated 0.2 μm filtered milli-Q water for 5 mins at 80 ℃. The weight of FM samples was weighted using a balance with the precision of 0.1 mg after drying (Mettler Toledo, China). Pristine FMs were performed as controls.

In parallel to the FM washing, the eluent was filtered through a 0.2 μm glass fiber membrane, the microplastics on the glass membrane were resuspended in saturated sodium chloride overnight to allow the microplastics floating on the liquid surface, and the supernatant was filtered again through a 0.2 μm CN/CA composite film membrane before the observation under a stereomicroscope. Triplicate pristine FMs and blanks were performed as controls.

2.3 Environmental parameters

Physiochemical parameters such as pH, temperature, and dissolved oxygen were measured *in situ* using a portable Water Quality Meter (SMAT, China). Salinity was measured using a hand-held practical salinity refractometer. Total organic matter (TOC) was measured using an Apollo 9000 Total Organic Carbon Analyzer (Teledyne Instruments Tekmar, USA) [28]. Additional environmental factors, such as nitrite (NO_2^-), nitrate (NO_3^-), and inorganic phosphate (PO_4^{3-}), were measured using a Discrete Chemistry Analyzer (CleverChem Anna, Germany) according to our previous methods [28]. To test the density of aged FMs, FM aliquots were placed into seawater with varying levels of salinities. When the FMs were suspended, their density matched that of the surrounding seawater.

2.4 Confocal microscopy and scanning electron microscopy

FM aliquots were fixed in a 2% glutaraldehyde solution overnight and rinsed with phosphate-buffered saline three times. For confocal microscopy, samples were stained with a 4,6-diamidino-2-phenylindole (DAPI) solution (final concentration: 50 μM, ZETA^{TM}) for 15

mins in the dark at ambient temperature before confocal microscopy observations (Nikon, Japan). The 405 nm laser was used for the excitation and visualization of DAPI signals. The Z-Step size was set to 1 µm to get regularly spaced cross-sections.

For the scanning electron microscopy, the fixed and rinsed aliquots were further dehydrated with a series of 75% ethanol, 90% ethanol, 100% ethanol, and 100% acetone for 15 minutes in respective solutions, followed by an air-drying process in a fume hood [25]. Samples were coated with a sputter coater and further observed under a scanning electron microscope (Hitachi, Japan).

2.5 Fourier transform infrared (FTIR) spectroscopy

FM aliquots were incubated in hydrogen peroxide (30%) to remove the biofilm [29]. Samples were washed with milli-Q water three times and dried in the fume hood. FM spectra were recorded using an FTIR spectrometer (PerkinElmer), using 16 scans from 4000 cm^{-1} to 400 cm^{-1}. The absorption band strength and polymer type identification were realized *via* Omnic Specta software (Thermo Fisher Scientific). To determine the aging process, the carbonyl index (CI) was calculated from the spectrum of the FMs. The CI value is usually used as a proxy of oxidation level of polymers, and can be obtained by calculating the adsorption of the ketone peak at 1715 cm^{-1} to the methylene peak at 1455 cm^{-1} [30].

2.6 DNA extraction and quantitative PCR (qPCR)

The microbial genomic DNA was extracted using the classical phenol-chloroform protocol from the outer layer of FMs (~ 5 cm^2), the swabs (stone controls), and the membrane filters (seawater controls) [31]. DNA quality and quantity were verified using NanoDrop One (Thermo Fisher), and the DNA integrity was checked on 1% agarose gel. The DNA concentration was quantified using a Qubit 3.0 fluorometer (Invitrogen).

To determine the total bacterial abundance in FMs, stones and seawater, bacterial 16S rRNA gene was quantified by qPCR using QuantStudio™ 5 Real-Time PCR System (Applied Biosystems) with ChamQ SYBR qPCR Master Mix and the bacterial specific primers (16S 338F, 5'-ACTCCTACGGGAGGCAGCA-3'; 806R 5'-GGACTACHVGGGTWTCTAAT-3'). The qPCR was conducted in 384-well plates with a 30 μL reaction mixture containing 15 μL qPCR Master Mix, 1 μL of each primer, and 1 μL template DNA. Standard curves were generated by 10-fold gradient diluted plasmid solutions. All samples were conducted in triplicates. The amplification efficiencies range from 85% to 105% in different PCR reactions ($R^2 > 0.995$) for the standard curve.

2.7 DNA sequencing, and data processing

Polymerase chain reaction (PCR) amplification was done to target the full-length 16S rRNA gene using universal small subunit ribosomal RNA (SSU rRNA) primers (27F, 5'-AGRGTTYGATYMTGGCTCAG-3'; 1492R, 5'-RGYTACCTTGTTACGACTT-3'). PacBio circular consensus sequencing (CCS) was performed for the 27 samples (Magigene Biotechnology, China), including triplicate samples from the three stations for FM, stone, and seawater samples. The PCR amplification profile included an initial denaturation of 15 min at 94 °C, followed by 27 cycles of denaturation at 95 °C for 30 s, annealing at 55 °C for 30 s, and amplification at 72 °C for 45 s, in addition to a final elongation step of 10 min at 72 °C. All the SSU rRNA data are available in the NCBI SRA repository (accession number PRJNA971390).

Processing of SSU rRNA sequences was performed using the QIIME2 microbiome bioinformatics platform [32]. The plugin UCLUST was used for clustering sequences at a threshold of 99% to define the operational taxonomic unit (OTU) [33]. OTUs were assigned against the Greengenes 13.8 database [34], and the OTUs affiliated to eukaryotes, archaea,

chloroplast, and mitochondria were removed. Alpha-diversity calculation and histogram visualization were realized with the MicrobiomeAnalyst server [35].

To quantify the degree of connectivity of microbial communities, a community metric 'cohesion' was calculated by integrating the relative bacterial abundance and the co-occurrence profile. For a given sample type (e.g., FMs), the cohesion is the summation of each OTU's negative coefficient to the rest OTUs, divided by that of the positive coefficient, and weight by bacterial abundance [36].

2.8 Pathogen identification and visualization

The bacterial pathogen list was obtained from the Enhanced Infectious Disease Database (EID2), which used an automated data mining process to extract information on pathogens and their hosts, and the pathogen-host interactions were verified by literature review [37]. Even though the bacterial pathogenicity was not strictly evidenced, the database was informative and widely used in recent studies [38,39]. The quality-controlled full-length 16S rRNA gene sequences in the pathogen list were retrieved from the EzBioCloud database [40]. To identify the pathogens in our samples, the PacBio sequencing data were blasted with the pathogen database with the criteria of sequence identity > 99%, E-value < $1 \times 10^{-10,}$ and coverage > 1300 bp [41]. To compare and assess the performance of the Illumina next-generation sequencing in identifying pathogens, the variable regions V4-V5 were extracted from the full-length 16S rRNA gene from the PacBio sequencing, and the used primers were specified from the previous study [11].

Pathogen sequences were aligned using the MAFFT [42], and the phylogenetic tree was constructed using the FastTree [43] and visualized using the iTOL [44].

2.9 Bacterial assembly process

In microbial ecology, both the stochastic (e.g., dispersal and drift) and the deterministic (e.g., environment selection) processes were important for their contributions to the bacterial community assembly [45]. To determine the importance of the stochastic process to microbial community assembly, the Sloan neutral model was constructed by predicting the occurrence of the OTUs in a local sample and the metacommunity (e.g., all FM samples) [46]. In the model, death, growth, and dispersal rates of OTUs were assumed to be equivalent. Thus, the model considers that the stochastic process drives the microbial assembly of a sample. A single free parameter, *m*, is a random loss of an OTU in a local community that would be replaced by the dispersal from the metacommunity and can be interpreted as a proxy of dispersal potential. The calculations were performed with the MicEco R package.

The relative importance of the stochastic and deterministic processes was quantified using the null model analysis. In brief, the observed taxa were divided into different groups (so-called 'bins') based on their phylogenetic relationships. The process governing each bin was quantified based on the phylogenic diversity using the beta Net Relatedness Index (βNRI) and taxonomic β-diversities using the Bray-Curtis-based Raup-Crick metric (RC). In terms of the deterministic process, the homogenous selection usually resulted in communities more similar, which was in contrast to the heterogeneous selection. Therefore, for each bin, the pairwise comparison of βNRI value of > 1.96 or < -1.96 suggested the phylogenetic turnover is greater than the null expectation and was regarded as the heterogenous and homogeneous selection, respectively. Subsequently, taxonomic β-diversities (i.e., RC) further partition the stochastic process when the absolute value of βNRI was less than 1.96. The pairwise comparisons with RC > 0.95 are regarded as dispersal limitation, while those < 0.95 as homogenizing dispersal. The remaining process (i.e., $|\beta\ \mathrm{NRI}| \leq 1.96$ and $|\mathrm{RC}| \leq 0.95$) represented the percentage of drift, weak selection, diversification, and/or week dispersal and was designated as "drift" hereafter. The fraction of the ecological processes in each bin was

weighted by their relative abundance and summarized at the community level. The triplicates of each sample type were averaged, before the quantification of the ecological processes using the iCAMP R package [47]. In addition, to decipher the assembly process of the pathogenic and non-pathogenic bacteria from FMs, stones, and seawater, those were extracted from the total bacterial community.

2.10 Statistical analyses

An unweighted-pair group method with arithmetic (UPGMA) dendrogram based on the Bray-Curtis similarities was used to visualize beta diversity. A similarity profile test (SIMPROF, PRIMER 6) was performed on the null hypothesis that a specific sub-cluster can be recreated by permuting the entry species and samples. The significant branch was used as a prerequisite for defining a bacterial cluster. Bacterial community difference was tested using permutational multivariate analysis of variance (PERMANOVA) [48], and the homogeneity of variances was respected using the *betadisper* test of the vegan R package. The student's t-test was performed using GraphPad Prism 9, and further adjusted with the Benjamini-Hochberg method to reduce the false discovery rate (FDR) at 5%. The redundancy analysis was performed using the vegan R package.

3 Results

3.1 Biofouling and physiochemical properties of FMs after exposure

FMs were exposed to the coastal water for two months from three stations *in situ*, representing different anthropogenic influences, including an open-water station at a distance of 200 m distance from the coast, a bay with intensive aquaculture (around 4 km^2), and the Shenzhen Bay (around 70 km^2) that is semi-enclosed by the metropolis in China (Shenzhen), with 17 million inhabitants (designated as S1, S2, and S3 hereafter) (Figure 1). After 2

months of exposure, the aging process of FMs was assessed, and the microbial community profiles and pathogen identification were characterized mainly based on the PacBio sequencing results.

Station S3 had higher concentrations of total organic matter (TOC), nitrite (NO_2^-), nitrate (NO_3^-), and inorganic phosphate (PO_4^{3-}) compared to S2, followed by S1 (Table S1). These results indicated that station S3 was more impacted by human activity. The three stations' temperature, pH, salinity, and dissolved oxygen were around 20.1 ± 1.2 ℃, 8.2 ± 0.1, 33 ± 1.9 PSU, and 7.8 ± 1.1 mg/L (Table S1).

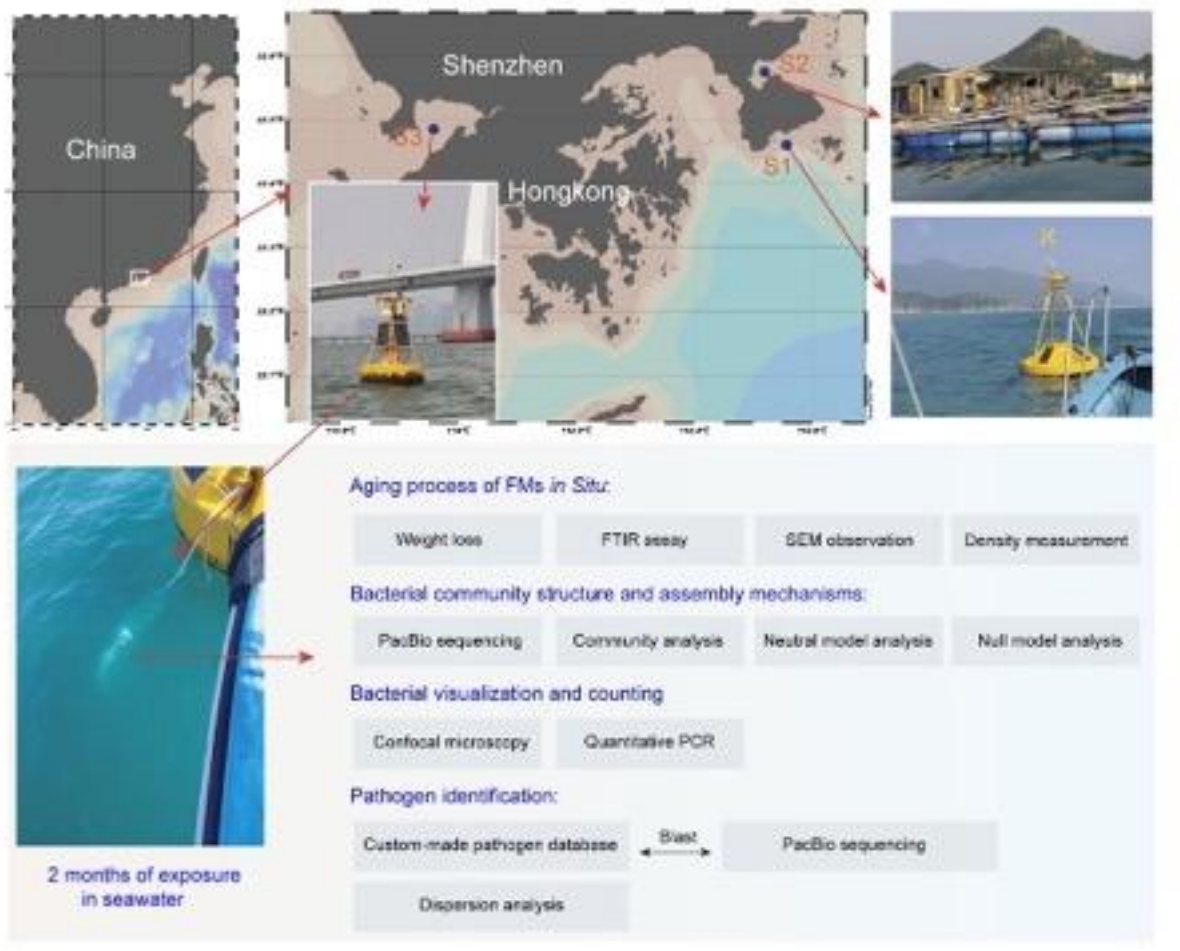

Figure 1. Experimental design. Schematic representation of the FM exposure and research methods, consisting of the assessment of the FM aging process *in situ*, bacterial community profiling, and pathogen identification.

After 2 months of incubation, the FMs' colors changed from blue (pristine, Figure 2a) to grey because of biofouling (Figure 2b-d). Additionally, high biofouling was visually observed in S2 compared to S1 and S3 (Figure 2b-d). A wide array of marine organisms was observed on FMs after the exposure. Amphipods (*Gammarus* sp.) and barnacles (*Balanus amphitrite*) colonized FMs from all stations (Figure 2 e-h). Mussels (*Perna viridis*) were found in the S1, with five individuals in maximum observed in one FM's surface (Figure 2i). FMs in S2 had severe biofouling by macroorganisms consisting of seaweeds (*Gelidium amansii*) and tube-forming serpulid worms (*Hydroides elegans*) (Figure 2c).

FM deterioration was observed from the S1, S3, and to a lesser extent, S2. For example, damages in FMs were visible after the exposure in S1 (Figure 2j). Besides, the broken microfibers were observed at the edges of the exterior shells of barnacles (Figure 2f). It seemed that microplastics and barnacle soft tissue were cross-linked (Figure 2g&h). To accurately measure the weight loss of the FMs after exposure, the biofilm of FMs was removed with a rigorous nitric acid digestion process. Triplicate samples from S1 and pristine controls were used for the analyses. The decoloring effect was observed for the pristine (Figure 2k) and the aged FMs (Figure 2l). The colors changed from blue to white. In addition, elastic ear bands were dissolved after the acid digestion. After washing and drying, 3% of weight loss was detected for the aged compared to the pristine one (t-test, $p < 0.05$), i.e., 70 mg of microplastics released into the ocean from a single FM. The surface topography of FMs has switched from flat (pristine one, Figure 2m) to rough (aged one, Figure 2n). Microplastics were detected for the aged FMs after the acid digestion (Figure 2o). The colonization of microorganisms on the FM surface was observed using the confocal microscope. As expected, bacteria-like structures were appeared in all FMs from the three stations and mainly patchily distributed on the FM surface (Figure 2p-r). In specific areas, the dense bacterial morphotypes formed aggregates, developing biofilm-like structures. Hence,

the distribution of the bacteria on the FM surface was heterogeneous. The bacterial abundances in FMs were further counted, which reached 1.9×10^6 (Standard deviation, i.e., SD = 1.9×10^6), 1.4×10^6 (SD = 4.9×10^5), and 2.9×10^6 (SD = 4.3×10^5) cells/cm^2 for the FMs in the station S1, S2, and S3, respectively. By contrast, the bacterial abundance was determined using quantitative PCR with specific primers for the FMs, stones, and seawater samples. The bacterial abundances of FM samples were 7.6×10^3 (SD = 9.2×10^3), 1.3×10^4 (SD = 2.2×10^4), and 7.8×10^4 (SD = 4.2×10^4) cells/cm^2 in the station S1, S2, and S3, respectively. Therefore, the bacterial abundance of FMs measured by the confocal microscopy was higher than that of qPCR.

For the qPCR results of the stones and seawater samples, the bacterial abundances of stone samples were 1.4×10^4 (SD = 1.6×10^4), 3.9×10^3 (SD = 2.2×10^3), and 3.3×10^4 (SD = 4.8×10^4) cells/cm^2 in the station S1, S2, and S3, respectively. No significant difference was found between the FMs and stone samples ($p > 0.05$). The bacterial abundances of seawater samples were 9.5×10^4 (SD = 6.0×10^4), 4.0×10^5 (SD = 9.5×10^4), and 8.1×10^4 (SD = 4.4×10^4) cells/mL for the seawater in the station S1, S2, and S3, respectively.

Due to the formation of the biofilm, the density of the FMs has been increased after the 2-month exposure. The density of FMs was determined for their outer layers from station S1. We found that FM aliquots can be suspended in seawater at a salinity of 17 (Figure 2s), for which the density was around 1.02 g/cm^3. The salinity of the three stations was between 31 and 35 (Table S1). Therefore, the released microplastics can be floated in the marine environment.

The results from scanning electron microscopy (SEM) showed that the diameter of the outer layer of fibers was around 20 μm. A smooth surface was observed for the pristine FMs (Figure 3 a-b). By contrast, cracks and rough surfaces appeared for the aged ones (Figure 3 c-

h). Dense bacteria-like structures were found in the aged FMs after exposure. Besides, a flake structure was found in S2 and could be a thick layer of a microbial mat.

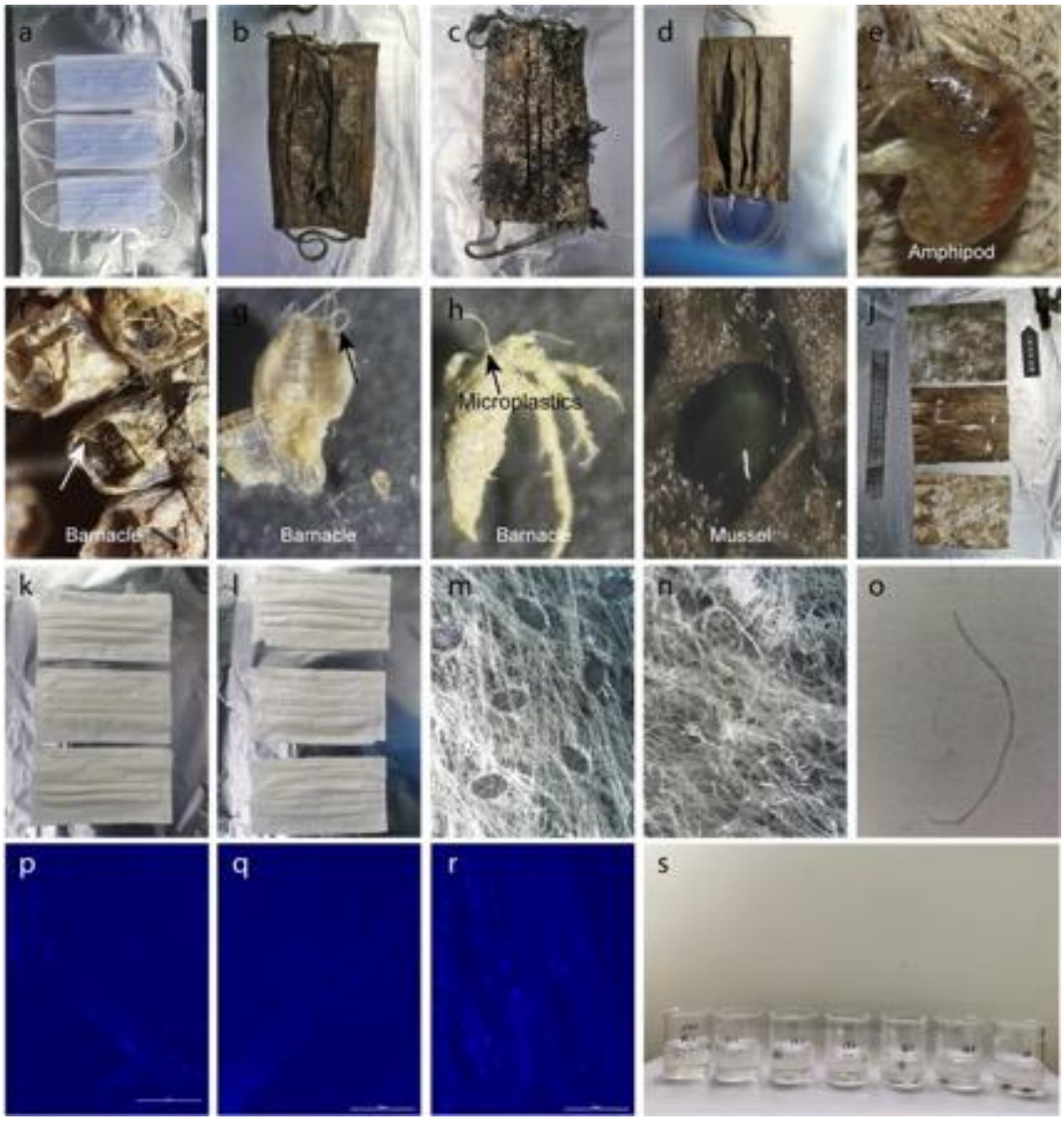

Figure 2. Biofouling and surface deterioration of FMs. Panel a represented the pristine FMs. Panels b-d represented FMs after 2 months of exposure from station S1, station S2, and station S3, respectively. Panels e-f represented amphipod (*Gammarus* sp.) and barnacles (*Balanus amphitrite*) that were found at all stations. Panels g-h represented the soft tissue of barnacles. Panel i represented mussels (*Perna viridis*) that were found in the S1. Panel j represented damages in the three layers of FMs after the

exposure. Panel k and l represented the pristine and weathered FMs after the treatment of the acid digestion process. Panel m and n represented the observation of pristine and weathered FMs using the stereomicroscope. Panel p represented the microplastic released from FMs. Arrows in panels g-h represented microplastics. Panels p-r represented confocal microscopy observation of FMs after the DAPI staining. The scale bars were 50 μm. Panel s represented the density measurement of FM aliquots.

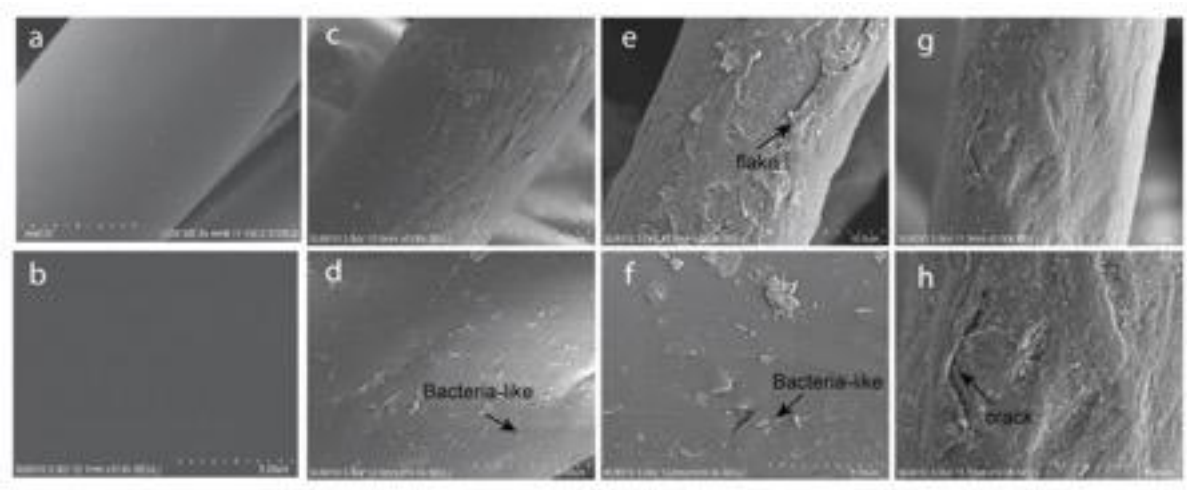

Figure 3. Scanning electron microscopy observation of FMs. Panels a and b represented pristine FMs. Panels c and d represented aged FMs from S1. Panels e and f represented aged FMs from S2. Panels g and h represented aged FMs from S3.

FTIR was used to identify the chemical composition of the FMs. For the pristine FMs, the three layers were made of polypropylene and the elastic ear bands were made of polyamide 6 (Figure S1 a-b), which was susceptible to acid digestion, as mentioned above. The outer layer of pristine FMs was subjected to a hydrogen dioxide process, exhibiting good resistance (Figure S1 b-c). No novel functional groups were observed for the aged FMs after the hydrogen dioxide process (Figure S1 d-f). The carbonyl groups around 1715 cm^{-1} can be used as the proxy of oxidation levels, which were not visually observed from FTIR spectra of pristine and aged FMs. The values of carbonyl index (CI) of the pristine and aged FMs were 0.38 ± 0.03 (pristine FMs), 0.37 ± 0.01 (aged FMs from S1), 0.39 ± 0.01 (aged FMs from S2),

and 0.33 ± 0.03 (aged FMs from S3), respectively. No differences were found for the pairwise comparisons of the CI value between the pristine FMs and the aged FMs (t-test, $p > 0.05$), indicating that the FMs did not undergo photodegradation.

Loosely attached microplastics were extracted from the FMs after ten rounds of ultrasonic baths. It turned out that the aged FMs (Figure 2o) released more microplastics than the pristine ones (64 fibers *versus* 18 fibers) (t-test, $p < 0.05$). Assuming each layer of FMs contributed equally to the weight loss, which was 70 mg, and with a diameter of 20 μm (as indicated in Figure 3), the average length of the released microplastics was calculated to be 889 μm (measured after acid digestion). With a density of polypropylene at 0.9 g/cm^3, it was estimated that one FM could potentially release up to 9×10^4 microplastic items during exposure in the marine environment.

3.2 Bacterial community dynamics

PacBio sequencing generated 542,589 sequence tags, falling into 6090 OTUs after randomly resampling to the lowest number of sequencing tags of 7041 at a 99% similarity threshold. No difference was found in the observed species between them (t-test, $p > 0.05$). The bacterial community differences were revealed in other alpha diversity indices. The indices of the Chao1 richness and the Shannon diversity were higher in the seawater compared to FMs (t-test, $p < 0.05$) (Figure 4a).

UPGMA dendrogram showed that biofilms formed on FMs and black agate stones differed from seawater samples (SW), with strong dissimilarity observed between these two clades (> 99%). For all the FMs and stone samples, the driving force of bacterial community structure was shaped by the geographical origins (Dissimilarity of 94% between S1 and (S2 and S3)), and to a lesser extent, by the material types (Dissimilarity of 74-86% between FMs and the stones) (Figure 4b). The PERMANOVA results confirmed significant differences among

sample types (plastisphere and seawater, $p < 0.01$) or sample stations (S1, S2, and S3, $p < 0.01$). The environment parameters were used to detect the variance of the bacterial community, and the redundancy analysis showed that less than 3% of the variance could be explained for FMs, stones, or seawater.

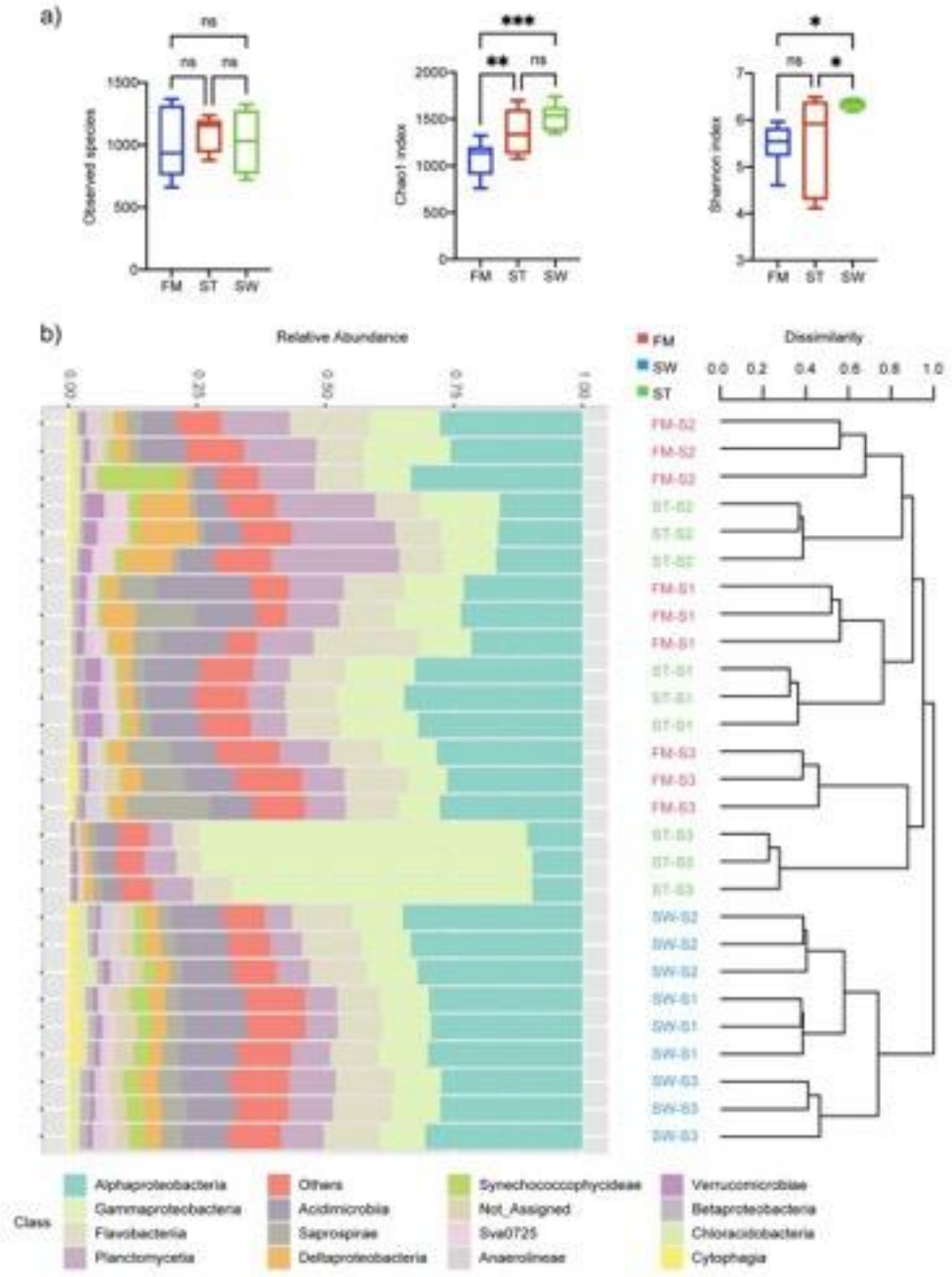

Figure 4. Illustration of bacterial alpha diversity (a) and comparison of taxonomic relative abundances and community structure of bacteria on the biofilm of FMs, stones (ST), and seawater (SW) by

cumulative bar charts comparing relative abundances (left) and by UPGMA dendrogram based on Bray–Curtis dissimilarities between 16S rRNA-based sequencing profiles (right) (b). Samples were collected from three stations: an open water station (S1), an aquafarm (S2), and a semi-enclosed bay of a metropolis (S3). Each sample type was performed in triplicates. P values less than 0.05, 0.01, and 0.001 were designated with one, two, and three asterisks, respectively.

Taxonomical analyses confirmed the specificity of the community structure in terms of sample types. The microbial community was dominated by Alphaproteobacteria and Flavobacteriia for FM samples (25.8 ± 3.9% and 12.8 ± 4.6%, respectively), Alphaproteobacteria and Gammaproteobacteria for stone samples (19.6 ± 10.8% and 30.5 ± 20.6%, respectively), and Alphaproteobacteria and Acidimicrobiia for seawater samples (30.9 ± 3.6% and 11.2 ± 1.4%, respectively). The difference in the class level was significant for specific taxa. For example, Alphaproteobacteria had a higher proportion in seawater samples than in FMs or stone samples (FDR < 0.05) (Figure 4b). We further investigated the top 3 OTUs in each sample type (Fig. S2). *Pseudomonas azotoformans* and an unclassified OTU of Bacteroidetes were particularly dominant for the FM samples. *Aliiroseovarius halocynthiae*, *Rhodopirellula* sp., and *Psychrobacter nivimaris* were more abundant in stone samples. By contrast, two unclassified OTUs of Rhodobacteraceae were more abundant in seawater samples.

3.3 Bacterial pathogen compositions

A bacterial pathogen list was constructed from the Enhanced Infectious Disease Database (EID2), containing 2252 bacterial species, which have been shown to infect a broad spectrum of hosts, such as humans, fish, plants, and some invertebrates (Table S2-11). The pathogen sequences were extracted from the EzBioCloud database, which provided standardized 16S rRNA sequences between the two most popular PCR primers (27F-1492R), which are the

same as the ones used in the PacBio sequencing. The PacBio sequencing results were blasted to the curated pathogen database, and a total of 191 sequences had significant alignments, assigned to 70 pathogen species. FMs and stones had a higher putative pathogen prevalence compared to seawater samples, with 21, 67, and 4 pathogen species found in the three sample types, respectively (5%, 27%, and 0.01% of the average relative abundance) (Figure 5). Besides, a phylogenetic tree was constructed for the pathogen species with a relative abundance higher than 0.1% in a sample type (Figure 5). Three pathogen species were specifically detected in FM samples. *Ralstonia pickettii* were more abundant in the plastisphere of FM samples (0.15%) than that in stone samples or seawater ($p < 0.05$). It is noteworthy that *Ralstonia pickettii* was not found in stone or seawater samples and could infect a wide range of species, such as humans and arthropods. Besides, *Bacillus amyloliquefaciens* and *Pseudomonas poae* were specifically detected in the FM samples (0.018% and 0.007%, respectively). For the two pathogen species, *Bacillus amyloliquefaciens* can infect plants and arthropods, and *Pseudomonas poae* can infect plants and birds. Moreover, sixteen pathogen species were detected in FM and controls, such as *Acinetobacter johnsonii* (0.01% in FM samples, pathogen of arthropods, plants, humans, fish, and green algae), *Brevundimonas diminuta* (0.01% in FM samples, pathogen of arthropods, plants, and humans), *Delftia lacustris* (0.01% in FM samples, pathogen of arthropods), *Enterobacter hormaechei* (0.01% in FM samples, pathogen of arthropods, plants, humans, and fish), *Escherichia fergusonii* (0.01% in FM samples, pathogen of arthropods and plants), *Exiguobacterium indicum* (0.004% in FM samples, pathogen of arthropods and fish), *Exiguobacterium profundum* (0.004% in FM samples, pathogen of arthropods and plants), *Limnobacter thiooxidans* (0.05% in FM samples, pathogen of plants), *Pseudomonas azotoformans* (0.06% in FM samples, pathogen of plants), *Pseudomonas costantinii* (3.5% in FM samples, pathogen of fungi), *Psychrobacter cibarius* (0.01% in FM samples, pathogen of

humans), *Roseovarius aestuarii* (0.03% in FM samples, pathogen of green algae), *Ruegeria atlantica* (0.03% in FM samples, pathogen of porifera), *Stenotrophomonas maltophilia* (0.004% in FM samples, pathogen of cnidaria, porifera, arthropods, plants, humans and others), *Tenacibaculum aestuarii* (0.03% in FM samples, pathogen of Mollusca), *Turicibacter sanguinis* (0.01% in FM samples, pathogen of humans), *Vibrio brasiliensis* (0.02% in FM samples, pathogen of arthropods), *Vibrio owensii* (0.01% in FM samples, pathogen of mollusca) (Table S12). By contrast, *Psychrobacter nivimaris* was extremely enriched in the biofilm of the stone samples ($p < 0.05$) (Figure 5).

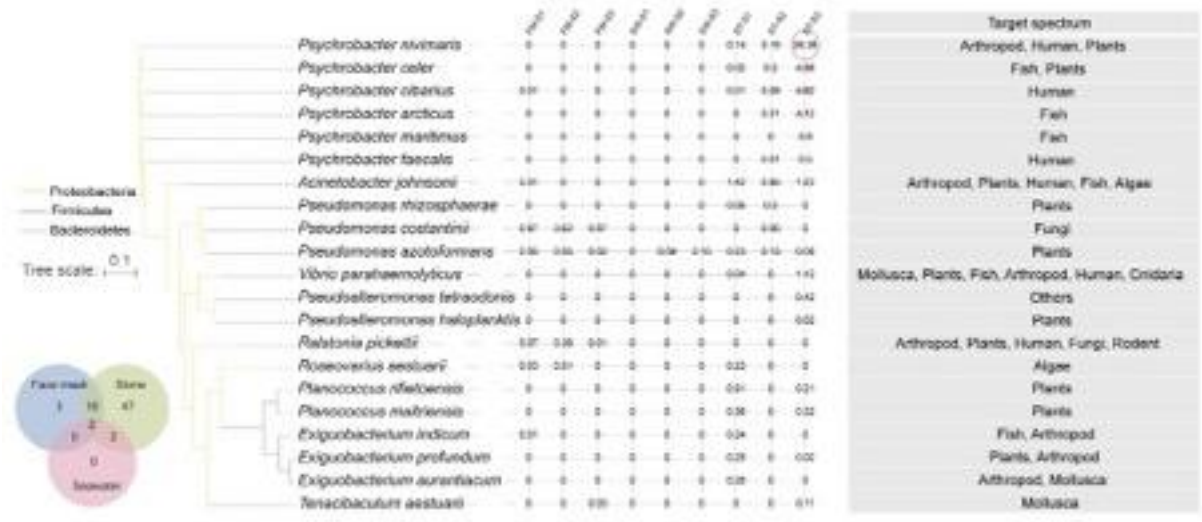

In order to evaluate the performance of PacBio sequencing in identifying pathogens, the V4-V5 variable regions of the 16S rRNA genes were extracted, which were widely used for the Illumina next-generation sequencing, and yielded 94.8% of the total sequences that fit the primers. After the extracted sequences (V4-V5 regions) were blasted to the pathogen database, we found 291 positive hits (> 407 bp). Therefore, the Illumina next-generation sequencing produced false discoveries, 34% of the taxa were not identified by the PacBio sequencing, indicative of a higher resolution in pathogen identification using the PacBio sequencing.

Figure 5. Pathogens identified by the PacBio full-length 16S rRNA sequencing. The phylogenetic tree was constructed for pathogens with relative abundances higher than 0.1% in a sample type. The branch colors represented taxonomies at the phylum level. Bubble size represented the relative abundance. The Venn plot showed the number of specific and shared OTUs within different sample types. The right panel showed the pathogen target spectra.

3.4 Community assembly processes

The Sloan neutral model was used to better explore the importance of stochastic processes in determining bacterial community assembly (Figure 6a). Based on the R^2 value (0.44, 0.41, and 0.47 for FMs, stones, and seawater, respectively) and the occurrences of the OTUs within the model prediction (89%, 88%, and 86% for FMs, stones, and seawater, respectively), the results indicated that the microbial communities in FMs, stones, and seawater were well described by the neutral model, and the stochastic processes are very important in shaping the bacterial community assembly. The *m* value was higher in seawater samples than in the stones or FM samples, indicating a higher dispersion potential for the seawater samples. The relative importance of different assembly processes was further classified, and it turned out that dispersion limitation was the main driver for the FMs and stone samples, whereas homogenous selection and dispersion limitation for the seawater samples (Figure 6b). In detail, the assembly processes of non-pathogenic and pathogenic bacteria in the plastisphere of FMs were further determined. As a subpopulation, it showed that the assembly processes of the non-pathogenic bacterial assembly process are similar to that of the total bacterial community from the plastisphere. However, the assembly process of pathogens from the plastisphere is dominated by homogeneous selection and less impacted by the dispersion limitation (Figure 6b). Variations were also found between the non-pathogenic and pathogenic bacteria in stones and seawater samples (Figure 6b).

The cohesion index was calculated to determine the stability of the microbial community. No significant difference was found between FMs and stone samples (0.64 *versus* 0.66). However, the cohesion value of FMs is significantly lower than that of seawater (0.64 *versus* 0.84) ($p < 0.05$), indicating that the microbial community in FMs is less stable than that in seawater (Figure 6c).

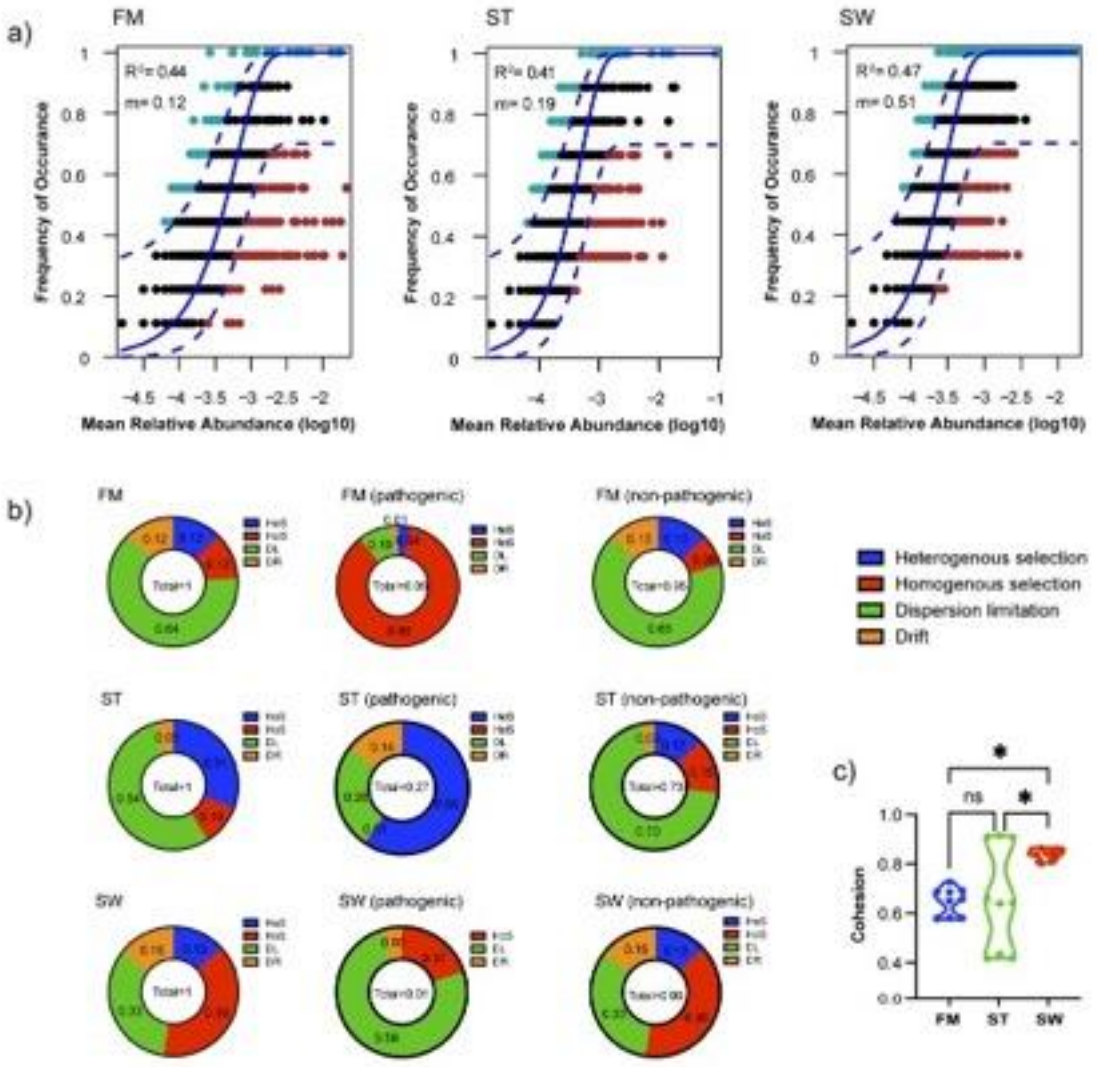

Figure 6. Bacterial community parameters depicted by the neutral community model (a), the null model analysis (b), and the cohesion results (c). In panel a, dots represented OTUs that occurred more or less frequently predicted by the neutral model. The predicted occurrence frequency was shown as the solid blue line, and the dashed blue line indicated the 95% confidence interval. The R^2 indicated

509 the fit to the model, and the *m* value indicated the migration potential of the metacommunity. The
510 values at the center of the circles of panel b represented the relative bacterial abundance.

511

4 Discussion

4.1 A methodology developed for pathogen identification in the plastisphere of FMs

A growing number of studies have been conducted to assess the influence of the plastisphere on marine ecosystems, and the pathogens were of increasing concern. We summarized 25 studies illustrated in two recent reviews concerning marine plastisphere-associated pathogens [21,49], and it showed that about 70% of studies adopted the technique of second-generation sequencing, which is characterized by short reads (less than 500 base pairs in general), usually targeted at viable regions of V3-V4 or V4-V5 of the 16S rRNA gene (Table S13) [50,51]. However, the resolution of pathogen classification of this technique was low and generally at the genus level, making it difficult to know the exact pathogen species. Instead, some studies adopted other techniques, such as bacterial isolation [52], selective medium [53], and fluorescence in situ hybridization (FISH). These techniques improved the accuracy. However, information was limited to specific pathogen types (Table S13) [54]. Previously, it has been shown that PacBio circular consensus sequencing could provide a near-zero error rate in the measurement of full-length 16S rRNA [55], which, in turn, can provide the taxonomic resolution of bacterial communities at the species level [56]. Therefore, it is plausible to use PacBio circular sequencing for putative pathogen identification. Herein, we constructed the pathogen database containing a wide range of hosts (e.g., humans, fish, plants) [37], and pathogen sequences were retrieved from the EzBioCloud database [40]. After alignments between the PacBio circular sequencing data and the pathogen database, we detected 70 putative pathogen species. *Vibrio* spp., as serious conditional pathogens from marine environments, attracted great attention in the plastisphere (Table S13) [57]. In our study, two *Vibrio* species, i.e., *Vibrio brasiliensis* (0.01%) and *Vibrio owensii* (0.004%) in the plastisphere were identified, served as pathogens for arthropods [58] and corals [59],

536 respectively, and may have an effect on marine creatures. The results also showed selective
537 enrichments of pathogens in the plastisphere, such as *Ralstonia pickettii*. It is noteworthy that
538 *Ralstonia pickettii* is a hydrocarbonoclastic bacterium [60,61]. Therefore, the labile organic
539 matter from FMs may promote pathogen growth, and FMs can provide a new niche for those
540 pathogens, as suggested from previous study [62].

541 Additionally, previous studies widely performed pathogen identification *via* alignments (i.e.,
542 BLAST [41]) between the Illumina sequencing data and their pathogen database at a 99%
543 similarity threshold [63–65]. To evaluate its performance, we extracted the V4-V5 regions of
544 16S rRNA genes from our PacBio data, representing the Illumina sequencing result. We
545 found that 34% of taxa (determined using V4-V5 regions of 16S rRNA gene) were not
546 detected in our pathogen results (PacBio full-length of 16S rRNA), indicating that the
547 Illumina sequencing will overestimate the pathogen results.

548 The PacBio sequencing can provide an advantage in pathogen detection compared to the
549 traditional isolation method in the case of bacteria with unusual phenotypic profiles, rare
550 bacteria, slow-growing bacteria, uncultivable bacteria, and the pathogen complex [66]. While
551 there were some limitations to this technique in discriminating bacterial species with close
552 phylogenetic relationships, which shared high similarity for their 16S rRNA genes (e.g.,
553 some species of *Bacillus* spp. and *Streptococcus* spp. elaborated from previous study) [67].
554 Nevertheless, there is great promise for PacBio sequencing to be applied to pathogen
555 identification, regardless of environmental surveillance or clinical microbiology laboratories.

556 *4.2 Deterioration of FMs and its impact on the bacterial communities of the plastisphere*

557 A significant number of microplastics can be released to the environment, aggravating
558 current environment plastic pollution [68–70]. Many broken microfibers were located at the
559 edges of the exterior shells of barnacles (*Balanus amphitrite*), indicative of biotic

deterioration processes, probably resulting from mechanical abrasion (Figure 2). In parallel, abiotic deterioration played an important role in FM deterioration, and much roughness was observed on the FM surface after exposure (Figure 2 and Figure 3). The technique of FTIR can be used to identify polymer types and assess the relative levels of polymer surface oxidation [71]. FMs showed the appearance of a carbonyl band of the FTIR spectra after simulating the sunlight aging [72]. On the contrary, this study showed the absence of a characteristic carbonyl band, suggesting that the photo degradation of plastic is relatively slow in marine environments. In the laboratory, pristine FMs can release hundreds to millions of microplastics after shaking or stirring [73]. In our condition, we found a 3% weight loss for FMs, which could be similar to the real condition because the pristine FMs were performed as the controls in parallel. By examining the hydrologic condition Field [75], we found that the water flow can reach 0.3 m/s for station S1 during the winter, indicating that such a water flow can lead to FM deterioration. During this study, it is estimated that up to 9 $\times 10^4$ can be released into the marine environment. The results could be overestimated, and the mechanical abrasion can lead to the formation of the pills and decrease the number of microplastics released from the fabrics [74].

The formation of biofilm can increase the plastic density [75]. The bulk FMs with the macroorganisms (e.g., barnacles) were found to be sinking in seawater (data not shown). However, a salinity of 17 can make the FM aliquots (without macroorganisms) suspended in this work, suggesting that the released microplastics from this study were floated in the surface ocean. Indeed, a recent study underlines that the deterioration of sinking plastics can result in smaller pieces regaining buoyancy and returning to the surface [76]. Therefore, FMs can have impacts on pelagic and benthic environments.

From this study, it is inferred that the bacterial communities in the plastisphere will change as microplastic transport through different oceanographic areas. Initially, the detached microplastics from FMs can have similar bacterial and pathogen compositions to those on FMs. Our previous study showed that polymer size or shape had no significant impact on the bacterial composition in the plastisphere [11]. Subsequently, along with the microplastic transport, the alterations of the bacterial community were expected. First, the richness and cohesion indices of bacterial communities were calculated and used as a proxy for bacterial stability [77,78]. The Chao1 richness and cohesion results were lower in FMs than in seawater, indicating bacteria in the plastisphere were less stable under environmental change (i.e., microplastic transport). Second, our study showed that geography could significantly impact the bacterial community in the plastisphere, which was supported by previous studies [79,80]. Therefore, changes in bacterial communities of the plastisphere can occur during microplastic transport. On the other hand, microplastic transport in the marine environment can result in bacterial dispersion because of the changes in the environmental conditions [24].

4.3 Rational basis of microplastics serving as vectors for pathogen transport

Reports on whether pathogens preferentially colonize plastics over other materials in the environment remain inconsistent, which is likely due to the variable environmental conditions of each study, with the environmental factors often having a stronger influence on plastisphere diversity than the polymer type [19,20,81]. The *Vibrio* spp. and *Pseudomonas* spp. were frequently reported from the previous studies in the marine environment [49]. Except for human pathogens, many pathogens can infect other marine organisms. Therefore, a comprehensive pathogen database, such as the one constructed in this study, will promote risk assessment for human beings and ecosystems. For this study, pathogens were investigated on FMs in comparison to stones and seawater controls. We found a high prevalence of putative pathogens in FMs compared to seawater (21 taxa in FMs *versus* 4 taxa

608 in seawater). In addition, the putative pathogens in the natural biofilm were characterized in
609 coastal stones. Selective enrichments were found in both FMs and stone samples, and there
610 was a low prevalence of the pathogens in FMs compared to stone samples (21 taxa in FMs
611 *versus* 67 taxa in stones). These results suggested that the pathogen's lifestyle preferred
612 living in the biofilm of FMs or stones during the winter season. However, the role of FMs
613 serving as pathogen vectors cannot be neglected. First, the marine environment was
614 considered the final reservoir of the plastics [82]. A higher prevalence of putative pathogens
615 on FMs than in seawater indicated that FMs and other plastic debris could be hotspots for the
616 pathogens in the coastal water and, in a broader context, in the open ocean. Second, selective
617 enrichments can be found in FMs as compared to stones or seawater samples. Moreover,
618 microplastics released from the FMs can be vectors for pathogen transport in marine
619 environments, which is not the situation for pathogens in coastal natural biofilm formed on
620 stones.

621 There is growing concern about the possibility that pathogens can be transported in the
622 plastisphere in the marine environment [21]. The assembly mechanism was clarified to infer
623 the pathogenic bacterial response during microplastic transport. The assembly process of the
624 pathogens from the plastisphere showed that homogeneous selection explained 85% of the
625 total ecological processes. Indeed, the homogenous selection is an indicator that the
626 pathogens were mainly influenced by the same environment selection, resulting in similar
627 compositions among different stations [45]. A relatively low dispersion limitation (10%) also
628 indicated that the majority of the putative pathogen could be transported along the coast (100
629 km in this study) without the occurrence of pathogen dispersion (bacteria escape from the
630 plastisphere).

The released microplastics can serve as vectors for transferring pathogens from the plastisphere to the organisms [83]. Previous studies showed that microbes living within the biofilm are highly beneficial and can become more infectious than when free-living [21]. Moreover, microplastics in the form of microfibers can be released from FMs. Fish species were found to ingest and retain the microfibers in their tissues (*Boops boops*, *Cathorops agassizii*) [84,85]. In fact, oyster *Saccostrea cucullata* at station S3 had an average of 8 microplastic items per individual, mainly in the form of microfiber [86]. This ingestion of microplastics by marine organisms may lead to diseases in those organisms and impact human health from the trophic transfer [87]. Besides, since many beaches were located near station S1, the microplastics released from FMs may create a new route for pathogen infection in humans.

Concluding Remarks

The chemical composition of the face masks was mainly made of polypropylene. After two months of exposure to the marine environment, a wide array of microorganisms and macroorganisms colonized the surface of face masks. Pathogens in the face masks were investigated using the PacBio sequencing of the 16S rRNA marker gene, showing its applicability to identify the pathogens at the species level. PacBio sequencing can be used as a main or auxiliary method in detecting pathogen species in many contexts, such as aquaculture and wastewater treatment. This study found the enrichment of the putative pathogens in the plastisphere of FMs compared to seawater in a subtropical coastal environment with intensive human activity. However, the relative abundance of putative pathogens in the plastisphere was less than in the coastal stones. Therefore, to conclude whether the FMs or the plastic litter is a reservoir of pathogens, its profiles in the open ocean are needed and warrant further studies. Even though the classification of pathogens at the

species level has greatly improved the accuracy, the pathogenicity should be revealed in future.

In accordance with other laboratory studies, we found severe deterioration of FMs after exposure, which could be an important source of microfibers in the marine environment. The FM aliquots can be suspended at a density of approximately 17 PSU, making the released microfibers transport potentially in the surface ocean. Our results also showed that assembly processes were distinct for the pathogenic and non-pathogenic bacteria, and the microfibers were favorable for transporting specific pathogens in the marine environment, which can increase the possibility of microbial invasion. In general, the occurrence of pathogens in nature had spatial and temporal patterns, long-term observations of the pathogen profile together with the host fitness may significantly advance the environmental epidemiology in this field.

Supporting Information

Figure S1 shows the spectra of the Fourier transform infrared spectroscopy. Figure S2. shows the relative abundance of the top 3 OTUs in each sample type using the bubble plot. Table S1 shows the physiochemical parameters of the seawater. Table S2-11 shows the putative pathogens for humans, fish, plants, arthropods, algae, fungi, Mollusca, Cnidaria, rodents, and others. Table S12 shows the relative abundance of the putative pathogens and their target spectra. Table S13 shows methods used for pathogen identifications from previous studies.

Acknowledgments

We are grateful to Shenzhen Langcheng Industry Company Ltd for their support on the work of FM exposure at buoys, and to Y.S. for the insightful comments on the manuscript. This work was supported by the NSFC (42077227 and 41976126), GuangDong Basic and Applied

Basic Research Foundation (Grant No. 2022A1515110519), the S&T Projects of Shenzhen Science and Technology Innovation Committee (Grant No. RCJC20200714114433069, JCYJ20200109142818589, and KCXFZ20201221173211033), the Shenzhen-Hong Kong-Macau Joint S&T Project (SGDX20220530111204028), and the Project of Shenzhen Municipal Bureau of Planning and Natural Resources (Grant No. [2021]735-927), as well as the "Anti-COVID19 Special Funding of Tsinghua SIGS" (JC2022020).

Reference

[1] Q. Jiang, Z. Xu, H. Zhang, Global impacts of COVID-19 on sustainable ocean development, The Innovation. 3 (2022) 100250. https://doi.org/10.1016/j.xinn.2022.100250.

[2] J.C. Prata, A.L.P. Silva, T.R. Walker, A.C. Duarte, T. Rocha-Santos, COVID-19 Pandemic Repercussions on the Use and Management of Plastics, Environ. Sci. Technol. 54 (2020) 7760–7765. https://doi.org/10.1021/acs.est.0c02178.

[3] S. Dharmaraj, V. Ashokkumar, S. Hariharan, A. Manibharathi, P.L. Show, C.T. Chong, C. Ngamcharussrivichai, The COVID-19 pandemic face mask waste: A blooming threat to the marine environment, Chemosphere. 272 (2021) 129601. https://doi.org/10.1016/j.chemosphere.2021.129601.

[4] M.R. Cordova, I.S. Nurhati, E. Riani, Nurhasanah, M.Y. Iswari, Unprecedented plastic-made personal protective equipment (PPE) debris in river outlets into Jakarta Bay during COVID-19 pandemic, Chemosphere. 268 (2021) 129360. https://doi.org/10.1016/j.chemosphere.2020.129360.

[5] R. Akhbarizadeh, S. Dobaradaran, I. Nabipour, M. Tangestani, D. Abedi, F. Javanfekr, F. Jeddi, A. Zendehboodi, Abandoned Covid-19 personal protective equipment along the Bushehr shores, the Persian Gulf: An emerging source of secondary microplastics in coastlines, Marine Pollution Bulletin. 168 (2021) 112386. https://doi.org/10.1016/j.marpolbul.2021.112386.

[6] H. Chowdhury, T. Chowdhury, S.M. Sait, Estimating marine plastic pollution from COVID-19 face masks in coastal regions, Marine Pollution Bulletin. 168 (2021) 112419. https://doi.org/10.1016/j.marpolbul.2021.112419.

[7] X. Chen, X. Chen, Q. Liu, Q. Zhao, X. Xiong, C. Wu, Used disposable face masks are significant sources of microplastics to environment, Environmental Pollution. 285 (2021) 117485. https://doi.org/10.1016/j.envpol.2021.117485.

[8] H. Liang, Y. Ji, W. Ge, J. Wu, N. Song, Z. Yin, C. Chai, Release kinetics of microplastics from disposable face masks into the aqueous environment, Science of The Total Environment. 816 (2022) 151650. https://doi.org/10.1016/j.scitotenv.2021.151650.

[9] Z. Wang, C. An, X. Chen, K. Lee, B. Zhang, Q. Feng, Disposable masks release microplastics to the aqueous environment with exacerbation by natural weathering, Journal of Hazardous Materials. 417 (2021) 126036. https://doi.org/10.1016/j.jhazmat.2021.126036.

[10] E.R. Zettler, T.J. Mincer, L.A. Amaral-Zettler, Life in the "Plastisphere": Microbial Communities on Plastic Marine Debris, Environmental Science & Technology. 47 (2013) 7137–7146. https://doi.org/10.1021/es401288x.

[11] J. Cheng, J. Jacquin, P. Conan, M. Pujo-Pay, V. Barbe, M. George, P. Fabre, S. Bruzaud, A. Ter Halle, A.-L. Meistertzheim, J.-F. Ghiglione, Relative Influence of Plastic Debris Size and Shape, Chemical Composition and Phytoplankton-Bacteria Interactions in Driving Seawater Plastisphere Abundance, Diversity and Activity, Front. Microbiol. 11 (2021) 610231. https://doi.org/10.3389/fmicb.2020.610231.

[12] R.J. Wright, G. Erni-Cassola, V. Zadjelovic, M. Latva, J.A. Christie-Oleza, Marine Plastic Debris: A New Surface for Microbial Colonization, Environ. Sci. Technol. 54 (2020) 11657–11672. https://doi.org/10.1021/acs.est.0c02305.

[13] M. Enfrin, J. Lee, Y. Gibert, F. Basheer, L. Kong, L.F. Dumée, Release of hazardous nanoplastic contaminants due to microplastics fragmentation under shear stress forces, Journal of Hazardous Materials. 384 (2020) 121393. https://doi.org/10.1016/j.jhazmat.2019.121393.

[14] Y. Zheng, J. Zhu, J. Li, G. Li, H. Shi, Burrowing invertebrates induce fragmentation of mariculture Styrofoam floats and formation of microplastics, Journal of Hazardous Materials. 447 (2023) 130764. https://doi.org/10.1016/j.jhazmat.2023.130764.

[15] M. Steer, M. Cole, R.C. Thompson, P.K. Lindeque, Microplastic ingestion in fish larvae in the western English Channel, Environmental Pollution. 226 (2017) 250–259. https://doi.org/10.1016/j.envpol.2017.03.062.

[16] U. Cabrejos-Cardeña, G.E. De-la-Torre, S. Dobaradaran, S. Rangabhashiyam, An ecotoxicological perspective of microplastics released by face masks, Journal of Hazardous Materials. 443 (2023) 130273. https://doi.org/10.1016/j.jhazmat.2022.130273.

[17] A.S. Hui Li, P. Sathishkumar, M.L. Selahuddeen, W.M. Asyraf Wan Mahmood, M.H. Zainal Abidin, R.A. Wahab, M.A. Mohamed Huri, F. Abdullah, Adverse environmental effects of disposable face masks due to the excess usage, Environmental Pollution. 308 (2022) 119674. https://doi.org/10.1016/j.envpol.2022.119674.

[18] M. Sendra, A. Rodriguez-Romero, M.P. Yeste, J. Blasco, A. Tovar-Sánchez, Products released from surgical face masks can provoke cytotoxicity in the marine diatom Phaeodactylum tricornutum, Science of The Total Environment. 841 (2022) 156611. https://doi.org/10.1016/j.scitotenv.2022.156611.

[19] R.J. Wright, M.G.I. Langille, T.R. Walker, Food or just a free ride? A meta-analysis reveals the global diversity of the Plastisphere, ISME J. 15 (2021) 789–806. https://doi.org/10.1038/s41396-020-00814-9.

[20] S. Oberbeckmann, M. Labrenz, Marine Microbial Assemblages on Microplastics: Diversity, Adaptation, and Role in Degradation, Annual Review of Marine Science. 12 (2020) 209–232. https://doi.org/10.1146/annurev-marine-010419-010633.

[21] J. Bowley, C. Baker-Austin, A. Porter, R. Hartnell, C. Lewis, Oceanic Hitchhikers – Assessing Pathogen Risks from Marine Microplastic, Trends in Microbiology. 29 (2021) 107–116. https://doi.org/10.1016/j.tim.2020.06.011.

[22] F. Audrézet, A. Zaiko, G. Lear, S.A. Wood, L.A. Tremblay, X. Pochon, Biosecurity implications of drifting marine plastic debris: Current knowledge and future research, Marine Pollution Bulletin. 162 (2021) 111835. https://doi.org/10.1016/j.marpolbul.2020.111835.

[23] C. Osunla, A. Okoh, Vibrio Pathogens: A Public Health Concern in Rural Water Resources in Sub-Saharan Africa, IJERPH. 14 (2017) 1188. https://doi.org/10.3390/ijerph14101188.

[24] K.P. Rumbaugh, K. Sauer, Biofilm dispersion, Nat Rev Microbiol. 18 (2020) 571–586. https://doi.org/10.1038/s41579-020-0385-0.

[25] S. Oberbeckmann, M.G.J. Loeder, G. Gerdts, A.M. Osborn, Spatial and seasonal variation in diversity and structure of microbial biofilms on marine plastics in Northern European waters., FEMS Microbiol Ecol. 49 (2014) 478–492. https://doi.org/10.1111/1574-6941.12409.

[26] S. Oberbeckmann, B. Kreikemeyer, M. Labrenz, Environmental Factors Support the Formation of Specific Bacterial Assemblages on Microplastics, Front. Microbiol. 8 (2018) 2709. https://doi.org/10.3389/fmicb.2017.02709.

[27] F. Pfeiffer, E.K. Fischer, Various Digestion Protocols Within Microplastic Sample Processing—Evaluating the Resistance of Different Synthetic Polymers and the Efficiency of Biogenic Organic Matter Destruction, Front. Environ. Sci. 8 (2020) 572424. https://doi.org/10.3389/fenvs.2020.572424.

[28] S.-J. Zhang, Y.-H. Zeng, J.-M. Zhu, Z.-H. Cai, J. Zhou, The structure and assembly mechanisms of plastisphere microbial community in natural marine environment, Journal of Hazardous Materials. 421 (2022) 126780. https://doi.org/10.1016/j.jhazmat.2021.126780.

[29] Y. Matsuguma, H. Takada, H. Kumata, H. Kanke, S. Sakurai, T. Suzuki, M. Itoh, Y. Okazaki, R. Boonyatumanond, M.P. Zakaria, S. Weerts, B. Newman, Microplastics in Sediment Cores from Asia and Africa as Indicators of Temporal Trends in Plastic Pollution, Arch Environ Contam Toxicol. 73 (2017) 230–239. https://doi.org/10.1007/s00244-017-0414-9.

[30] L. Lyu, Z. Wang, M. Bagchi, Z. Ye, A. Soliman, A. Bagchi, N. Markoglou, J. Yin, C. An, X. Yang, H. Bi, M. Cai, An investigation into the aging of disposable face masks in landfill leachate, Journal of Hazardous Materials. 446 (2023) 130671. https://doi.org/10.1016/j.jhazmat.2022.130671.

[31] F. Marty, J.-F. Ghiglione, S. Païssé, H. Gueuné, L. Quillet, M.C.M. van Loosdrecht, G. Muyzer, Evaluation and optimization of nucleic acid extraction methods for the

molecular analysis of bacterial communities associated with corroded carbon steel, Biofouling. 28 (2012) 363–380. https://doi.org/10.1080/08927014.2012.672644.

[32] E. Bolyen, J.R. Rideout, M.R. Dillon, N.A. Bokulich, C.C. Abnet, G.A. Al-Ghalith, H. Alexander, E.J. Alm, M. Arumugam, F. Asnicar, Y. Bai, J.E. Bisanz, K. Bittinger, A. Brejnrod, C.J. Brislawn, C.T. Brown, B.J. Callahan, A.M. Caraballo-Rodríguez, J. Chase, E.K. Cope, R. Da Silva, C. Diener, P.C. Dorrestein, G.M. Douglas, D.M. Durall, C. Duvallet, C.F. Edwardson, M. Ernst, M. Estaki, J. Fouquier, J.M. Gauglitz, S.M. Gibbons, D.L. Gibson, A. Gonzalez, K. Gorlick, J. Guo, B. Hillmann, S. Holmes, H. Holste, C. Huttenhower, G.A. Huttley, S. Janssen, A.K. Jarmusch, L. Jiang, B.D. Kaehler, K.B. Kang, C.R. Keefe, P. Keim, S.T. Kelley, D. Knights, I. Koester, T. Kosciolek, J. Kreps, M.G.I. Langille, J. Lee, R. Ley, Y.-X. Liu, E. Loftfield, C. Lozupone, M. Maher, C. Marotz, B.D. Martin, D. McDonald, L.J. McIver, A.V. Melnik, J.L. Metcalf, S.C. Morgan, J.T. Morton, A.T. Naimey, J.A. Navas-Molina, L.F. Nothias, S.B. Orchanian, T. Pearson, S.L. Peoples, D. Petras, M.L. Preuss, E. Pruesse, L.B. Rasmussen, A. Rivers, M.S. Robeson, P. Rosenthal, N. Segata, M. Shaffer, A. Shiffer, R. Sinha, S.J. Song, J.R. Spear, A.D. Swafford, L.R. Thompson, P.J. Torres, P. Trinh, A. Tripathi, P.J. Turnbaugh, S. Ul-Hasan, J.J.J. van der Hooft, F. Vargas, Y. Vázquez-Baeza, E. Vogtmann, M. von Hippel, W. Walters, Y. Wan, M. Wang, J. Warren, K.C. Weber, C.H.D. Williamson, A.D. Willis, Z.Z. Xu, J.R. Zaneveld, Y. Zhang, Q. Zhu, R. Knight, J.G. Caporaso, Reproducible, interactive, scalable and extensible microbiome data science using QIIME 2, Nat Biotechnol. 37 (2019) 852–857. https://doi.org/10.1038/s41587-019-0209-9.

[33] R.C. Edgar, Search and clustering orders of magnitude faster than BLAST, Bioinformatics. 26 (2010) 2460–2461. https://doi.org/10.1093/bioinformatics/btq461.

[34] T.Z. DeSantis, P. Hugenholtz, N. Larsen, M. Rojas, E.L. Brodie, K. Keller, T. Huber, D. Dalevi, P. Hu, G.L. Andersen, Greengenes, a Chimera-Checked 16S rRNA Gene Database and Workbench Compatible with ARB, Appl Environ Microbiol. 72 (2006) 5069–5072. https://doi.org/10.1128/AEM.03006-05.

[35] J. Chong, P. Liu, G. Zhou, J. Xia, Using MicrobiomeAnalyst for comprehensive statistical, functional, and meta-analysis of microbiome data, Nature Protocols. 15 (2020) 799–821. https://doi.org/10.1038/s41596-019-0264-1.

[36] C.M. Herren, K.D. McMahon, Cohesion: a method for quantifying the connectivity of microbial communities, ISME J. 11 (2017) 2426–2438. https://doi.org/10.1038/ismej.2017.91.

[37] M. Wardeh, C. Risley, M.K. McIntyre, C. Setzkorn, M. Baylis, Database of host-pathogen and related species interactions, and their global distribution, Sci Data. 2 (2015) 150049. https://doi.org/10.1038/sdata.2015.49.

[38] R. Gibb, D.W. Redding, K.Q. Chin, C.A. Donnelly, T.M. Blackburn, T. Newbold, K.E. Jones, Zoonotic host diversity increases in human-dominated ecosystems, Nature. 584 (2020) 398–402. https://doi.org/10.1038/s41586-020-2562-8.

[39] G.F. Albery, C.J. Carlson, L.E. Cohen, E.A. Eskew, R. Gibb, S.J. Ryan, A.R. Sweeny, D.J. Becker, Urban-adapted mammal species have more known pathogens, Nat Ecol Evol. 6 (2022) 794–801. https://doi.org/10.1038/s41559-022-01723-0.

[40] S.-H. Yoon, S.-M. Ha, S. Kwon, J. Lim, Y. Kim, H. Seo, J. Chun, Introducing EzBioCloud: a taxonomically united database of 16S rRNA gene sequences and whole-genome assemblies, International Journal of Systematic and Evolutionary Microbiology. 67 (2017) 1613–1617. https://doi.org/10.1099/ijsem.0.001755.

[41] S.F. Altschul, W. Gish, W. Miller, E.W. Myers, D.J. Lipman, Basic Local Alignment Search Tool, Journal of Molecular Biology. 215 (1990) 403–410.

[42] K. Katoh, D.M. Standley, MAFFT Multiple Sequence Alignment Software Version 7: Improvements in Performance and Usability, Molecular Biology and Evolution. 30 (2013) 772–780. https://doi.org/10.1093/molbev/mst010.

[43] M.N. Price, P.S. Dehal, A.P. Arkin, FastTree 2 – Approximately Maximum-Likelihood Trees for Large Alignments, PLoS ONE. 5 (2010) e9490. https://doi.org/10.1371/journal.pone.0009490.

[44] I. Letunic, P. Bork, Interactive Tree Of Life (iTOL) v4: recent updates and new developments, Nucleic Acids Research. 47 (2019) W256–W259. https://doi.org/10.1093/nar/gkz239.

[45] J. Zhou, D. Ning, Stochastic Community Assembly: Does It Matter in Microbial Ecology?, Microbiol Mol Biol Rev. 81 (2017) e00002-17. https://doi.org/10.1128/MMBR.00002-17.

[46] W.T. Sloan, M. Lunn, S. Woodcock, I.M. Head, S. Nee, T.P. Curtis, Quantifying the roles of immigration and chance in shaping prokaryote community structure, Environ Microbiol. 8 (2006) 732–740. https://doi.org/10.1111/j.1462-2920.2005.00956.x.

[47] D. Ning, M. Yuan, L. Wu, Y. Zhang, X. Guo, X. Zhou, Y. Yang, A.P. Arkin, M.K. Firestone, J. Zhou, A quantitative framework reveals ecological drivers of grassland microbial community assembly in response to warming, Nat Commun. 11 (2020) 4717. https://doi.org/10.1038/s41467-020-18560-z.

[48] M.J. Anderson, Permutational Multivariate Analysis of Variance (PERMANOVA), Wiley StatsRef: Statistics Reference Online. (2017) 1–15. https://doi.org/10.1002/9781118445112.stat07841.

[49] M. Junaid, J.A. Siddiqui, M. Sadaf, S. Liu, J. Wang, Enrichment and dissemination of bacterial pathogens by microplastics in the aquatic environment, Science of The Total Environment. 830 (2022) 154720. https://doi.org/10.1016/j.scitotenv.2022.154720.

[50] C. Dussud, A.L. Meistertzheim, P. Conan, M. Pujo-Pay, M. George, P. Fabre, J. Coudane, P. Higgs, A. Elineau, M.L. Pedrotti, G. Gorsky, J.F. Ghiglione, Evidence of niche partitioning among bacteria living on plastics, organic particles and surrounding seawaters, Environmental Pollution. 236 (2018) 807–816. https://doi.org/10.1016/j.envpol.2017.12.027.

[51] Z. Wang, J. Gao, Y. Zhao, H. Dai, J. Jia, D. Zhang, Plastisphere enrich antibiotic resistance genes and potential pathogenic bacteria in sewage with pharmaceuticals, Science of The Total Environment. 768 (2021) 144663. https://doi.org/10.1016/j.scitotenv.2020.144663.

[52] M.M. Silva, G.C. Maldonado, R.O. Castro, J. de Sá Felizardo, R.P. Cardoso, R.M. dos Anjos, F.V. de Araújo, Dispersal of potentially pathogenic bacteria by plastic debris in Guanabara Bay, RJ, Brazil, Marine Pollution Bulletin. 141 (2019) 561–568. https://doi.org/10.1016/j.marpolbul.2019.02.064.

[53] A. Rodrigues, D.M. Oliver, A. McCarron, R.S. Quilliam, Colonisation of plastic pellets (nurdles) by E. coli at public bathing beaches, Marine Pollution Bulletin. 139 (2019) 376–380. https://doi.org/10.1016/j.marpolbul.2019.01.011.

[54] J.P. Harrison, M. Schratzberger, M. Sapp, A.M. Osborn, Rapid bacterial colonization of low-density polyethylene microplastics in coastal sediment microcosms, BMC Microbiology. 14 (2014) 232. https://doi.org/10.1186/s12866-014-0232-4.

[55] B.J. Callahan, J. Wong, C. Heiner, S. Oh, C.M. Theriot, A.S. Gulati, S.K. McGill, M.K. Dougherty, High-throughput amplicon sequencing of the full-length 16S rRNA gene with single-nucleotide resolution, Nucleic Acids Research. 47 (2019) e103–e103. https://doi.org/10.1093/nar/gkz569.

[56] J.S. Johnson, D.J. Spakowicz, B.-Y. Hong, L.M. Petersen, P. Demkowicz, L. Chen, S.R. Leopold, B.M. Hanson, H.O. Agresta, M. Gerstein, E. Sodergren, G.M. Weinstock, Evaluation of 16S rRNA gene sequencing for species and strain-level microbiome analysis, Nat Commun. 10 (2019) 5029. https://doi.org/10.1038/s41467-019-13036-1.

[57] K.D. Brumfield, M. Usmani, K.M. Chen, M. Gangwar, A.S. Jutla, A. Huq, R.R. Colwell, Environmental parameters associated with incidence and transmission of pathogenic *Vibrio spp* ., Environmental Microbiology. 23 (2021) 7314–7340. https://doi.org/10.1111/1462-2920.15716.

[58] G. Li, G. Xie, H. Wang, X. Wan, X. Li, C. Shi, Z. Wang, M. Gong, T. Li, P. Wang, Q. Zhang, J. Huang, Characterization of a novel shrimp pathogen, *Vibrio brasiliensis* , isolated from Pacific white shrimp, *Penaeus vannamei*, Journal of Fish Diseases. 44 (2021) 1543–1552. https://doi.org/10.1111/jfd.13475.

[59] B. Ushijima, A. Smith, G.S. Aeby, S.M. Callahan, Vibrio owensii Induces the Tissue Loss Disease Montipora White Syndrome in the Hawaiian Reef Coral Montipora capitata, PLoS ONE. 7 (2012) e46717. https://doi.org/10.1371/journal.pone.0046717.

[60] B. Morasch, H.H. Richnow, B. Schink, A. Vieth, R.U. Meckenstock, Carbon and Hydrogen Stable Isotope Fractionation during Aerobic Bacterial Degradation of Aromatic Hydrocarbons, Appl Environ Microbiol. 68 (2002) 5191–5194. https://doi.org/10.1128/AEM.68.10.5191-5194.2002.

[61] Y. Guo, Y. Liu, T. Xiang, J. Li, M. Lv, Y. Yan, J. Zhao, J. Sun, X. Yang, C. Liao, J. Fu, J. Shi, G. Qu, G. Jiang, Disposable Polypropylene Face Masks: A Potential Source of Micro/Nanoparticles and Organic Contaminates in Humans, Environ. Sci. Technol. 57 (2023) 5739–5750. https://doi.org/10.1021/acs.est.2c06802.

[62] F. Crisafi, F. Smedile, M.M. Yakimov, F. Aulenta, S. Fazi, V. La Cono, A. Martinelli, V. Di Lisio, R. Denaro, Bacterial biofilms on medical masks disposed in the marine environment: a hotspot of biological and functional diversity, Science of The Total Environment. 837 (2022) 155731. https://doi.org/10.1016/j.scitotenv.2022.155731.

[63] D. Zhu, J. Ma, G. Li, M.C. Rillig, Y.-G. Zhu, Soil plastispheres as hotpots of antibiotic resistance genes and potential pathogens, ISME J. (2021). https://doi.org/10.1038/s41396-021-01103-9.

[64] Q. Chen, X. An, H. Li, J. Su, Y. Ma, Y.-G. Zhu, Long-term field application of sewage sludge increases the abundance of antibiotic resistance genes in soil, Environment International. 92–93 (2016) 1–10. https://doi.org/10.1016/j.envint.2016.03.026.

[65] K. Yang, Q.-L. Chen, M.-L. Chen, H.-Z. Li, H. Liao, Q. Pu, Y.-G. Zhu, L. Cui, Temporal Dynamics of Antibiotic Resistome in the Plastisphere during Microbial Colonization, Environ. Sci. Technol. 54 (2020) 11322–11332. https://doi.org/10.1021/acs.est.0c04292.

[66] P.C.Y. Woo, S.K.P. Lau, J.L.L. Teng, H. Tse, K.-Y. Yuen, Then and now: use of 16S rDNA gene sequencing for bacterial identification and discovery of novel bacteria in clinical microbiology laboratories, Clinical Microbiology and Infection. 14 (2008) 908–934. https://doi.org/10.1111/j.1469-0691.2008.02070.x.

[67] D.L. Church, L. Cerutti, A. Gürtler, T. Griener, A. Zelazny, S. Emler, Performance and Application of 16S rRNA Gene Cycle Sequencing for Routine Identification of Bacteria in the Clinical Microbiology Laboratory, Clin Microbiol Rev. 33 (2020) e00053-19. https://doi.org/10.1128/CMR.00053-19.

[68] D. Tang Kuok Ho, Abundance of Microplastics in Wastewater Treatment Sludge, J. Hum. Earth Future. 3 (2022) 138–146. https://doi.org/10.28991/HEF-2022-03-01-010.

[69] L. Van, N. Abdul Hamid, Md.F. Ahmad, A.N.A. Ahmad, R. Ruslan, P.F. Muhamad Tamyez, Factors of Single Use Plastic Reduction Behavioral Intention, Emerg Sci J. 5 (2021) 269–278. https://doi.org/10.28991/esj-2021-01275.

[70] R. Ratnawati, R. Wulandari, A.C. Kumoro, H. Hadiyanto, Response Surface Methodology for Formulating PVA/Starch/Lignin Biodegradable Plastic, Emerg Sci J. 6 (2022) 238–255. https://doi.org/10.28991/ESJ-2022-06-02-03.

[71] G.E. De-la-Torre, A.D. Forero López, D.C. Dioses-Salinas, M.D. Fernández Severini, S. Dobaradaran, R. Madadi, M. Ben-Haddad, Microplastics released from face masks used during the COVID-19 pandemic: A review of the characterization techniques, TrAC Trends in Analytical Chemistry. 167 (2023) 117227. https://doi.org/10.1016/j.trac.2023.117227.

[72] C. Chen, G. Yu, B. Wang, F. Li, H. Liu, W. Zhang, Lifetime prediction of non-woven face masks in ocean and contributions to microplastics and dissolved organic carbon, Journal of Hazardous Materials. 441 (2023) 129816. https://doi.org/10.1016/j.jhazmat.2022.129816.

[73] H. Jiang, D. Luo, L. Wang, Y. Zhang, H. Wang, C. Wang, A review of disposable facemasks during the COVID-19 pandemic: A focus on microplastics release, Chemosphere. 312 (2023) 137178. https://doi.org/10.1016/j.chemosphere.2022.137178.

[74] T. Yang, M. Gao, B. Nowack, Formation of microplastic fibers and fibrils during abrasion of a representative set of 12 polyester textiles, Science of The Total Environment. 862 (2023) 160758. https://doi.org/10.1016/j.scitotenv.2022.160758.

[75] M. Kooi, E.H.V. Nes, M. Scheffer, A.A. Koelmans, Ups and Downs in the Ocean: Effects of Biofouling on Vertical Transport of Microplastics, Environ. Sci. Technol. 51 (2017) 7963–7971. https://doi.org/10.1021/acs.est.6b04702.

[76] L.A. Amaral-Zettler, E.R. Zettler, T.J. Mincer, M.A. Klaassen, S.M. Gallager, Biofouling impacts on polyethylene density and sinking in coastal waters: A macro/micro tipping point?, Water Research. 201 (2021) 117289. https://doi.org/10.1016/j.watres.2021.117289.

[77] D.J. Hernandez, A.S. David, E.S. Menges, C.A. Searcy, M.E. Afkhami, Environmental stress destabilizes microbial networks, ISME J. 15 (2021) 1722–1734. https://doi.org/10.1038/s41396-020-00882-x.

[78] H. Guo, P. Dong, F. Gao, L. Huang, S. Wang, R. Wang, M. Yan, D. Zhang, Sucrose addition directionally enhances bacterial community convergence and network stability of the shrimp culture system, Npj Biofilms Microbiomes. 8 (2022) 22. https://doi.org/10.1038/s41522-022-00288-x.

[79] S. Oberbeckmann, A.M. Osborn, M.B. Duhaime, Microbes on a bottle: Substrate, season and geography influence community composition of microbes colonizing marine plastic debris, PLoS ONE. 11 (2016) 1–24. https://doi.org/10.1371/journal.pone.0159289.

[80] J. Cheng, D. Xing, P. Wang, S. Tang, Z. Cai, J. Zhou, X. Zhu, Enrichment of Antibiotic Resistant Genes and Pathogens in Face masks from Coastal Environments, Journal of Hazardous Materials. (2023) 131038. https://doi.org/10.1016/j.jhazmat.2023.131038.

[81] R. Metcalf, D.M. Oliver, V. Moresco, R.S. Quilliam, Quantifying the importance of plastic pollution for the dissemination of human pathogens: The challenges of choosing an appropriate 'control' material, Science of The Total Environment. 810 (2022) 152292. https://doi.org/10.1016/j.scitotenv.2021.152292.

[82] A. Stubbins, K.L. Law, S.E. Muñoz, T.S. Bianchi, L. Zhu, Plastics in the Earth system, Science. 373 (2021) 51–55. https://doi.org/10.1126/science.abb0354.

[83] J. Cheng, A.-L. Meistertzheim, D. Leistenschneider, L. Philip, J. Jacquin, M.-L. Escande, V. Barbe, A. ter Halle, L. Chapron, F. Lartaud, S. Bertrand, H. Escriva, J.-F. Ghiglione, Impacts of microplastics and the associated plastisphere on physiological, biochemical, genetic expression and gut microbiota of the filter-feeder amphioxus, Environment International. 172 (2023) 107750. https://doi.org/10.1016/j.envint.2023.107750.

[84] F.E. Possatto, M. Barletta, M.F. Costa, J.A.I. do Sul, D.V. Dantas, Plastic debris ingestion by marine catfish: An unexpected fisheries impact, Marine Pollution Bulletin. 62 (2011) 1098–1102. https://doi.org/10.1016/j.marpolbul.2011.01.036.

[85] M.A. Nadal, C. Alomar, S. Deudero, High levels of microplastic ingestion by the semipelagic fish bogue Boops boops (L.) around the Balearic Islands, Environmental Pollution. 214 (2016) 517–523. https://doi.org/10.1016/j.envpol.2016.04.054.

[86] H.-X. Li, L.-S. Ma, L. Lin, Z.-X. Ni, X.-R. Xu, H.-H. Shi, Y. Yan, G.-M. Zheng, D. Rittschof, Microplastics in oysters Saccostrea cucullata along the Pearl River Estuary,

China, Environmental Pollution. 236 (2018) 619–625. https://doi.org/10.1016/j.envpol.2018.01.083.

[87] M. Carbery, W. O'Connor, T. Palanisami, Trophic transfer of microplastics and mixed contaminants in the marine food web and implications for human health, Environment International. 115 (2018) 400–409. https://doi.org/10.1016/j.envint.2018.03.007.